iScience

CellPress

Article

The Plasticity of Mesenchymal Stem Cells in Regulating Surface HLA-I

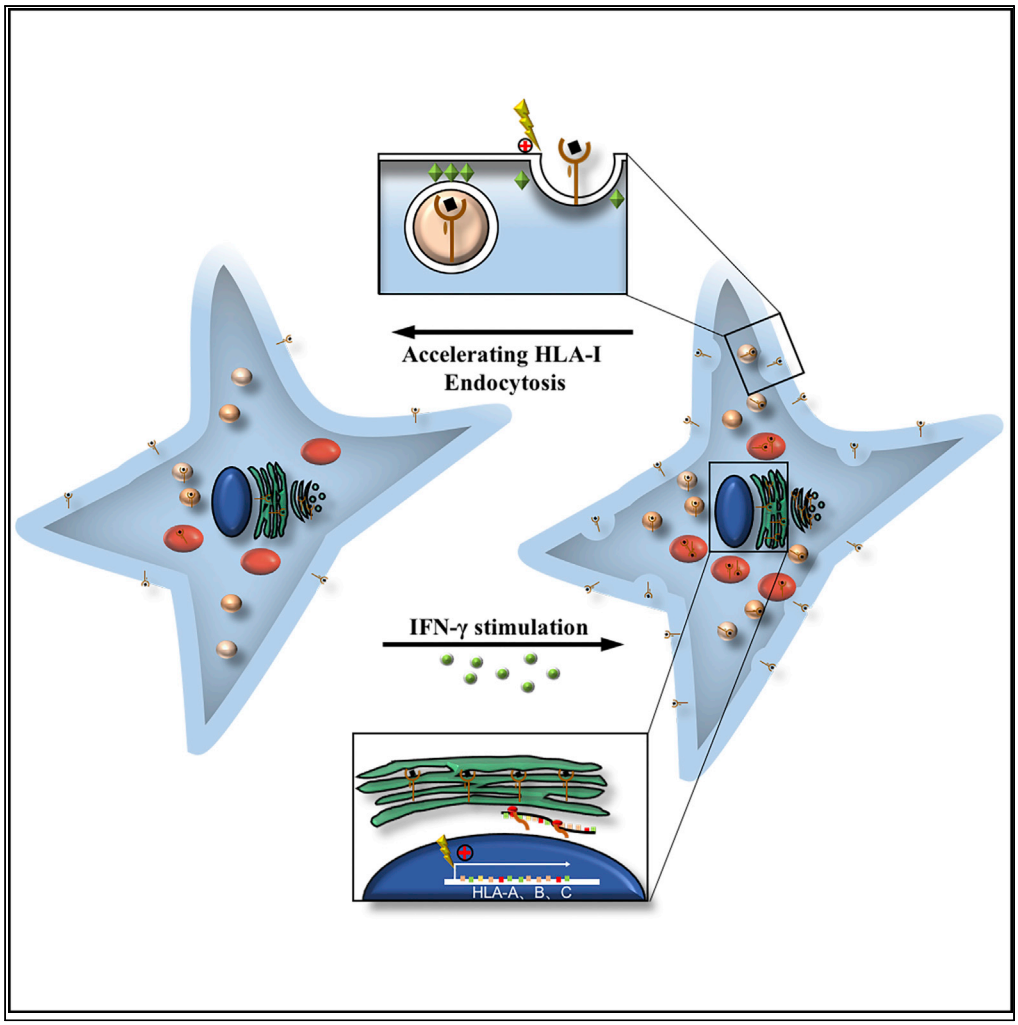

Yafei Wang, Jiayun Huang, Lin Gong, ..., Xiaohui Zou, Hongwei Ouyang, Hua Liu

liuhua@zju.edu.cn

HIGHLIGHTS

hESC-MSCs have the plasticity of maintaining low HLA-I expression on cell surface

hESC-MSCs downregulate the surface HLA-I expression through endocytosis of HLA-I

hESC-MSCs with lower HLA-I surface expression induce weaker MLR and slighter DTH

Wang et al., iScience 15, 66–78
May 31, 2019
https://doi.org/10.1016/j.isci.2019.04.011

iScience

CellPress

Article

The Plasticity of Mesenchymal Stem Cells in Regulating Surface HLA-I

Yafei Wang,[1,2] Jiayun Huang,[1,3,4] Lin Gong,[1,2] Dongsheng Yu,[5] Chenrui An,[1,2] Varitsara Bunpetch,[1,2] Jun Dai,[6] He Huang,[7,12] Xiaohui Zou,[8] Hongwei Ouyang,[1,2,9,10,11] and Hua Liu[1,2,13,*]

SUMMARY

A low surface expression level of human leukocyte antigen class I (HLA-I) ensures that the mesenchymal stem cells (MSCs) escape from the allogeneic recipients' immunological surveillance. Here, we discovered that both transcriptional and synthesis levels of HLA-I in MSCs increased continuously after interferon (IFN)-γ treatment, whereas interestingly, their surface HLA-I expression was downregulated after reaching an HLA-I surface expression peak. Microarray data indicated that the post-transcriptional process plays an important role in the downregulation of surface HLA-I. Further studies identified that IFN-γ-treated MSCs accelerated HLA-I endocytosis through a clathrin-independent dynamin-dependent endocytosis pathway. Furthermore, cells that have self-downregulated surface HLA-I expression elicit a weaker immune response than they previously could. Thus uncovering the plasticity of MSCs in the regulation of HLA-I surface expression would reveal insights into the membrane transportation events leading to the maintenance of low surface HLA-I expression, providing more evidence for selecting and optimizing low-immunogenic MSCs to improve the therapeutic efficiency.

INTRODUCTION

Polymorphisms in human leukocyte antigen (HLA) class I genes can cause the rejection of stem cells or tissue grafts in allogeneic recipients, which affects the safety and efficiency of therapies. Mesenchymal stem cells (MSCs) have been widely considered and reported to have therapeutic function in various degenerative and inflammatory diseases (Hosseini et al., 2018; Wang et al., 2016); so it is important to evaluate HLA-I expression on MSCs when considering about allogeneic MSC transplantation therapy. Although MSCs can be isolated from multiple tissues including bone marrow, adipose, and umbilical cord, only a very limited number of MSCs can be harvested from specific sources, generally requiring several weeks of *ex vivo* expansion to reach the demanding therapeutic MSC dose. In addition, they have been reported to exhibit large heterogeneity between different tissue sources and complicated donors' physical status in cell qualities following differentiation or immunomodulation abilities (Kim et al., 2018; Kunimatsu et al., 2018; Yang et al., 2018). Therefore pluripotent stem cells, such as induced pluripotent stem cells (iPSCs) and embryonic stem cells, were introduced as potential sources for MSCs due to their capacity to differentiate into the MSC lineage. However, iPSCs have the potential risks of chromosomal instability and oncogenic transformation associated with the application of viral vectors during the reprogramming process (Okita et al., 2007; Yu et al., 2007). In addition, it raised a concern that the reprogramming of iPSCs may be incomplete so that they still carry donor-specific characteristics, resulting in iPSCs with variable gene expression or DNA methylation (Chin et al., 2009; Doi et al., 2009). Thus, although allogeneic embryonic stem cells carry the risk of teratoma formation and face the challenge of maintaining genetic stability during long-term culture (Hentze et al., 2007), these cells have recently been proposed as an efficient source for MSC generation to provide high-quality "off-the-shelf" human embryonic stem cell-derived MSC (hESC-MSC) products (Hematti, 2011). Hence, hESC-MSCs must abide by a rigorous quality control system, evaluating their safety and immunogenicity during cell transplantation.

The immunogenicity of MSCs remains poorly defined and controversial. The prevailing dogma considers allogeneic MSCs as immune privileged or immune evasive. However, some studies showed the generation of alloantibodies and immune rejection after allogeneic MSC transplantation.

Culture-expanded MSCs have been confirmed by expressing a low level of surface HLA-I, no HLA-II, and costimulatory molecules including CD40, CD80, and CD86 (Klyushnenkova et al., 2005). Furthermore,

Continued

[1]Dr. Li Dak Sum & Yip Yio Chin Center for Stem Cell and Regenerative Medicine, Zhejiang University, School of Medicine, Hangzhou 310058, P.R.China

[2]Key Laboratory of Tissue Engineering and Regenerative Medicine of Zhejiang Province, Zhejiang University, School of Medicine, Hangzhou 310058, P.R.China

[3]Department of Orthopedic Surgery, 2nd Affiliated Hospital, Zhejiang University, School of Medicine, Zhejiang 310009, P.R.China

[4]Orthopaedics Research Institute of Zhejiang University, Zhejiang 310009, P.R.China

[5]Department of Orthopedics, Zhejiang Provincial People's Hospital, Hangzhou Medical College, Hangzhou, Zhejiang, 310014, P.R.China

[6]Department of Medical Genetics, Medicum, University of Helsinki, Helsinki 00290, Finland

[7]Bone Marrow Transplantation Center, The First Affiliated Hospital, Zhejiang University, School of Medicine, Hangzhou, Zhejiang 310003, P.R. China

[8]Central Laboratory, the First Affiliated Hospital, Zhejiang University, School of Medicine, Hangzhou, Zhejiang 310003, P.R.China

[9]Department of Sports Medicine, Zhejiang University, School of Medicine, Hangzhou 310058, P.R.China

[10]Zhejiang University-University of Edinburgh Institute & School of Basic Medicine, Zhejiang University, School of Medicine, Hangzhou 310003, P. R. China

MSCs were reported to be capable of producing a variety of immunomodulatory cytokines such as prostaglandin E2, interleukin10, transforming growth factor β, HLA-G, 2,3-dioxygenase, and inducible nitric oxide synthase, increasing the proportion of regulatory T cells and inhibiting the function of natural killer (NK) cells and effector T cells (Aggarwal and Pittenger, 2005). Some studies illustrated that allogeneic MSCs maintained low immunogenicity even after being immune challenged *in vitro*. In addition, when compared with the injection of peripheral blood mononuclear cells *in vivo*, allogeneic MSC injection did not elicit T cell proliferation and inflammatory cytokine secretion (Lee et al., 2014). Further evidence from Zangi et al. showed that the MSCs (20 days) were able to survive longer when compared with fibroblasts (10 days) in allogeneic host mice (Zangi et al., 2009). These results suggested that MSCs may exhibit lower immunogenicity than other differentiated cells and that MSCs can regulate themselves, as well as the environment, to maintain a hypo-immunogenic condition.

However, there also exist controversial reports regarding the immunogenicity of MSCs. It was reported that MSCs became highly immunogenic after being transplanted into the host (Yang et al., 2017); previous results indicated that allogeneic MSC injection stimulated the hosts' T cell response, which threatened MSC survival (Beggs et al., 2006). In addition, the ability of MSCs is often limited by the cell's poor engraftment rate, hindering their therapeutic efficiency, as well as the unknown route of MSC administration (Gu et al., 2015). Reviews by Ankrum et al. and Berglund et al. provided a thorough discussion on the immunogenicity of MSCs and insisted that it was worthwhile to consider MSC immunogenicity to improve the efficiency and safety of MSC therapies (Ankrum et al., 2014; Berglund et al., 2017). The rate of immune detection and elimination of allogeneic MSCs is dictated by the balance between a given cell's relative expression of immunogenic and immunosuppressive factors. Meanwhile, the cell cycle may also have an effect on the stem cells' immunogenicity. Agudo et al. have reported that the hair follicle stem cells (HFSCs) within the telogen phase (quiescent state) can downregulate the antigen presentation machinery to evade cellular immunity (Agudo et al., 2018). The cell state of MSCs can also be regulated into a quiescent state by altering the culture medium or plate as previously reported (Moya et al., 2017; Rumman et al., 2018), but a published microarray data reported that quiescent MSCs induced a stronger immune response in contrast (GO:0006954, PTSG2, IL10, IL1A, IL1B, CCR7) (Rumman et al., 2018). Thus it is still unknown whether it is beneficial to maintain MSCs in the quiescent phase to maintain low immunogenicity, especially low HLA-I expression. The alterations of MSCs' immunogenicity possibly depend on various factors including both the cell microenvironment and cell state. Therefore more studies need to be conducted to understand the details related to MSCs' immunogenicity, which could help improve the efficiency of MSC transplantation.

The major role of HLA-I is to act as an identifying card for all nucleated cells. In healthy individuals, all these molecules are autologous to avoid being attacked by $CD8^+$ T cells; however, when cells exhibit abnormal characteristics (e.g., cancer cells, allotransplantation, and viral infections), they express aberrant or non-self HLA-I molecules or antigens on their surface, rendering them to be targeted by $CD8^+$ T cells for destruction and elimination from the body to then be destroyed and eliminated from the body (Bjorkman et al., 1987). Meanwhile, cells that have HLA-I defects will be targeted by NK cells (Kollnberger, 2016); therefore HLA-I molecules are critical when considering allogeneic MSC transplantation.

The surface HLA-I expression level depends on both HLA-I presentation and HLA-I endocytosis. HLA-I antigen processing and presenting machinery (APM) is relatively similar among different cell types and is believed to contain several steps including protein breakdown, peptide transport, peptide trimming, HLA-I assembling, and HLA-I-peptide complex exportation; however, the internalization components of HLA-I vary between different cell types and status. In addition, because the HLA-I pathway gradually evolves to improve its detection and elimination of abnormal cells, tumor cells and some virus-infected cells have also coevolved and improved its cloaking mechanisms to avoid such detection. For example, the abnormalities of antigen processing and presentation in HLA-I are discovered in many types of cancers (Campoli et al., 2004), and a large majority of viruses have evolved ways to tamper with the APM or internalize HLA-I from the cell membrane (Hewitt, 2003). Nearly every step in the assembly and trafficking of HLA-I represents potential targets for ablating HLA-I expression on the cell surface. Nevertheless, it is still unknown how MSCs regulate their HLA-I expression.

The majority of immunogenicity studies on MSCs were carried out *in vitro*, and it should be noted that culture-expanded hMSCs typically express low levels of HLA-I on the surface, allowing them to evade immune surveillance. MSCs have been verified to have therapeutic functions in many inflammatory

[11]China Orthopedic Regenerative Medicine Group (CORMed), Hangzhou 310003, P.R. China

[12]Institute of Hematology, Zhejiang University, Hangzhou, Zhejiang 310003, P.R.China

[13]Lead Contact

*Correspondence: liuhua@zju.edu.cn

https://doi.org/10.1016/j.isci.2019.04.011

diseases such as osteoarthritis and autoimmune encephalitis; however, MSCs exposed to the inflammatory cytokine, interferon (IFN)-γ, can significantly express more HLA-I (Barrachina et al., 2016; Martini et al., 2010). Therefore we investigated the expression level of HLA-I on hESC-MSCs and examined its underlying regulatory mechanism, particularly in an inflamed microenvironment, hoping to better understand the immunogenicity of MSCs and improve the efficiency of MSC therapy.

RESULTS

MSCs Can Self-Downregulate Their HLA-I Surface Expression

In our previous study, characterization of MSC phenotype in the generated hESC-MSCs has been identified (Wang et al., 2017); here we aimed to study the expression of HLA-I on hESC-MSCs in an inflamed niche. IFN-γ is one of the common inflammatory cytokines, secreted mainly from cytotoxic T lymphocytes. It has been reported that IFN-γ can upregulate HLA-I expression on cancer cells, leading to the activation of tumor-specific immune response (Martini et al., 2010); however, it is still unclear whether IFN-γ treatment will have an effect on hESC-MSC HLA-I expression. In this study, we stimulated hESC-MSC with 100 U/mL IFN-γ for 0, 1, 2, and 3 days; qRT-PCR results demonstrated a continuous upregulation of polymorphic class I molecule (*HLA-A*, *HLA-B*, and *HLA-C*) expression in hESC-MSCs following IFN-γ stimulation (Figure 1A). In addition, western blot results also illustrated a more prominent HLA-I band with longer stimulation time, indicating that hESC-MSCs' total HLA-I protein level expression was upregulated in the presence of IFN-γ, where the intensity also increases over time (Figures 1B and 1C). In contrast, data analyzed by flow cytometry suggested a different expression outcome. Results illustrated that hESC-MSCs exhibited a degree of plasticity to maintain homeostasis; at day 1, the surface HLA-I expression on hESC-MSCs was first observed to be upregulated after IFN-γ stimulation, and then the expression was automatically downregulated (Figures 1D and 1E). When compared with hESC-MSCs, bone marrow MSCs exhibited weaker HLA-I autoregulation ability as the downregulation of HLA-I initiated at day 2 after IFN-γ stimulation (Figures S1A and S1B); therefore the surface HLA-I auto-downregulation ability varies between different sources of MSCs. Taken together, the presence of IFN-γ upregulates HLA-I expression level in hESC-MSCs; however, the cells are able to independently reverse the effect leading to the downregulation of HLA-I surface expression in the later stage.

Microarray Data Reveals the Transcriptional Changes in MSCs under IFN-γ Treatment

To investigate hESC-MSCs' underlying mechanism in the downregulation of HLA-I surface expression, we performed microarray analysis on IFN-γ-stimulated hESC-MSCs after 0, 1, and 3 days of stimulation (marked as Day0, Day1, Day3); a total of 3,054 differentially expressed genes were significantly regulated in these three groups (Figure 2A). According to the short time-series expression miner (STEM) analysis, the differential genes can be classified into eight groups (Figure 2B), where we further focused on the group (indicated as green background, N = 312 genes) that was continuously upregulated with IFN-γ treatment (Day3 > Day1 > Day0) (Figure 2C). Gene ontology enrichment analysis on this specific group was performed using DAVID; results indicated that these genes were not only highly related with the immune response but also enriched in terms associated with vesicle transportation and endocytosis pathway (Figure 2D, indicated as the red bar). Taken together, microarray data indicated that the vesicle transportation and endocytosis pathway may play an important role in regulating the hESC-MSCs' surface HLA-I expression after IFN-γ treatment.

MSCs Accelerate the Endocytosis of Surface HLA-I

The HLA-I surface expression level is regulated by the balance between the endoplasmic reticulum (ER)-Golgi-plasma membrane transportation rate and endocytosis transportation rate. Immunofluorescence was performed to determine the location of HLA-I in different organelles (ER, Golgi, endosome, and lysosome) on samples of Day0, Day1, and Day3. Results illustrated that the co-localization of HLA-I in ER was low both before and after IFN-γ stimulation, whereas HLA-I molecules co-localized in the Golgi, endosome, and lysosome were significantly upregulated after IFN-γ treatment (Figure 3A). Consistently, immunofluorescence intensity peaks of HLA-I (green line) were detected to be overlapped with Golgi, endosome, and lysosome intensity peak (red line) separately, but not with the ER intensity peak (red line) (Figure 3B). Quantitative analysis was also executed by measuring the co-localization rate with Mander's values ranging from 0 to 1, where bigger values indicate higher co-localization rate. Quantitative results suggested that the HLA-I co-localized in the Golgi, endosome, and lysosome of hESC-MSCs were all upregulated after IFN-γ treatment; furthermore, the HLA-I in endosome was significantly upregulated at Day3 when compared with Day1 (Figure 3C). Furthermore, flow cytometry was utilized to examine HLA-I

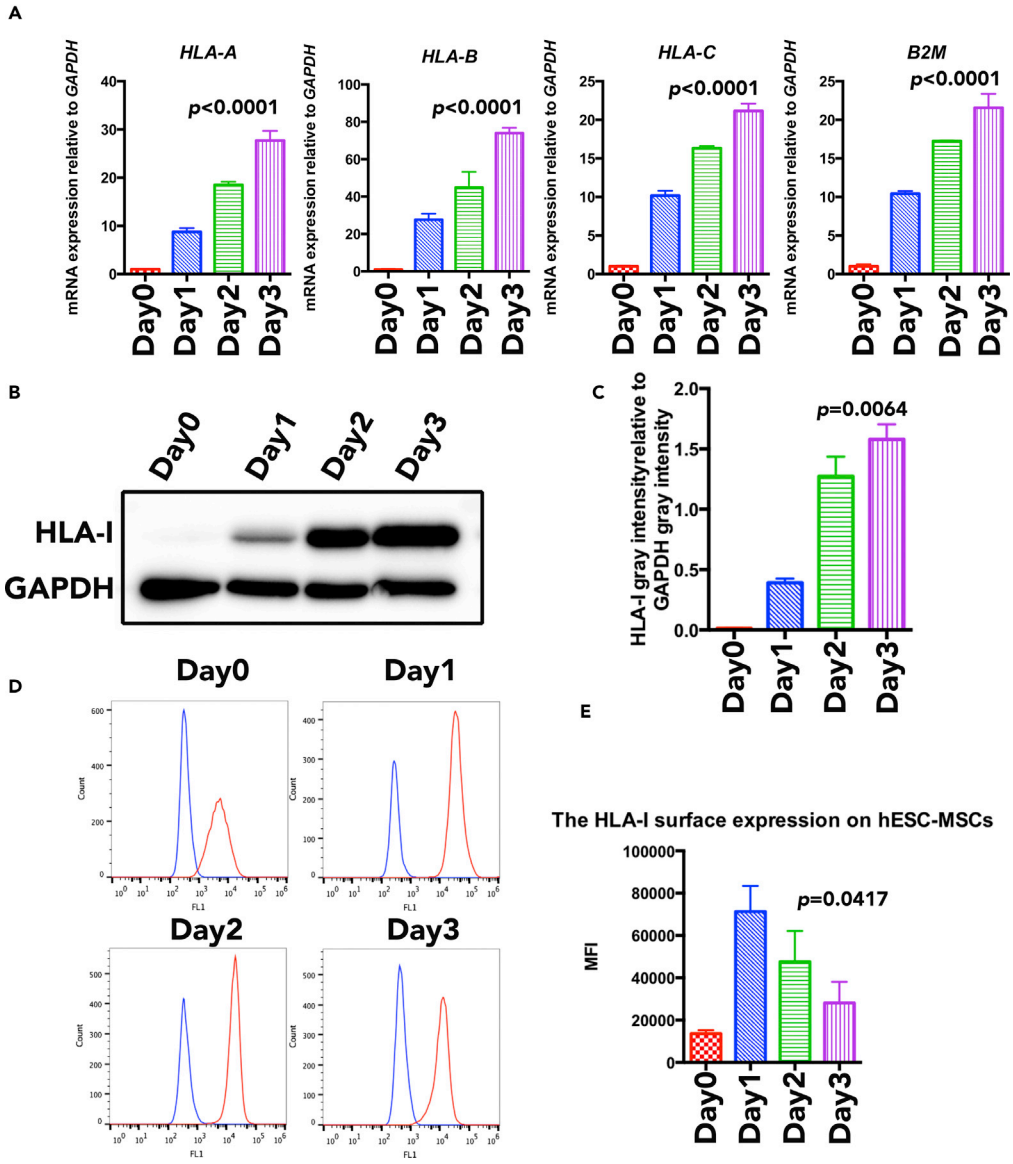

Figure 1. The HLA-I Expression of hESC-MSCs under IFN-γ Treatment

(A) qRT-PCR expression analysis of HLA-I-related genes (including HLA-A, HLA-B, HLA-C, and B2M) on hESC-MSCs under IFN-γ treatment. RNA expression levels were normalized to the level of GAPDH expression. Data are shown as means ± SEM.

(B) HLA-I expression on hESC-MSCs within IFN-γ treatment for 0 day, 1 day, 2 days, and 3 days were compared by western blot.

(C) The western blot results quantified analysis of HLA-I total expression level on hESC-MSCs within IFN-γ treatment for 0 day, 1 day, 2 days, and 3 days. HLA-I expression levels were normalized to the level of GAPDH expression. Data are shown as means ± SEM.

(D) HLA-I surface expression on hESC-MSCs (red line) within IFN-γ treatment for 0 day, 1 day, 2 days, and 3 days were compared by flow cytometry analysis. Blue line demarcates isotype control.

(E) The flow cytometry results quantified analysis of HLA-I surface expression level on hESC-MSCs with IFN-γ treatment for 0 day, 1 day, 2 days, and 3 days by mean fluorescence index. Data are shown as means ± SEM.

See also Figures S1–S6.

endocytosis rate in hESC-MSCs; results revealed that the HLA-I surface expression on hESC-MSCs was significantly upregulated after IFN- γ stimulation; however, it also showed faster endocytosis rate to down-regulate surface HLA-I (Figure 3D). On the whole, these data demonstrated that hESC-MSCs upregulate the plasma HLA-I endocytosis rate as a mechanism to reduce HLA-I surface expression.

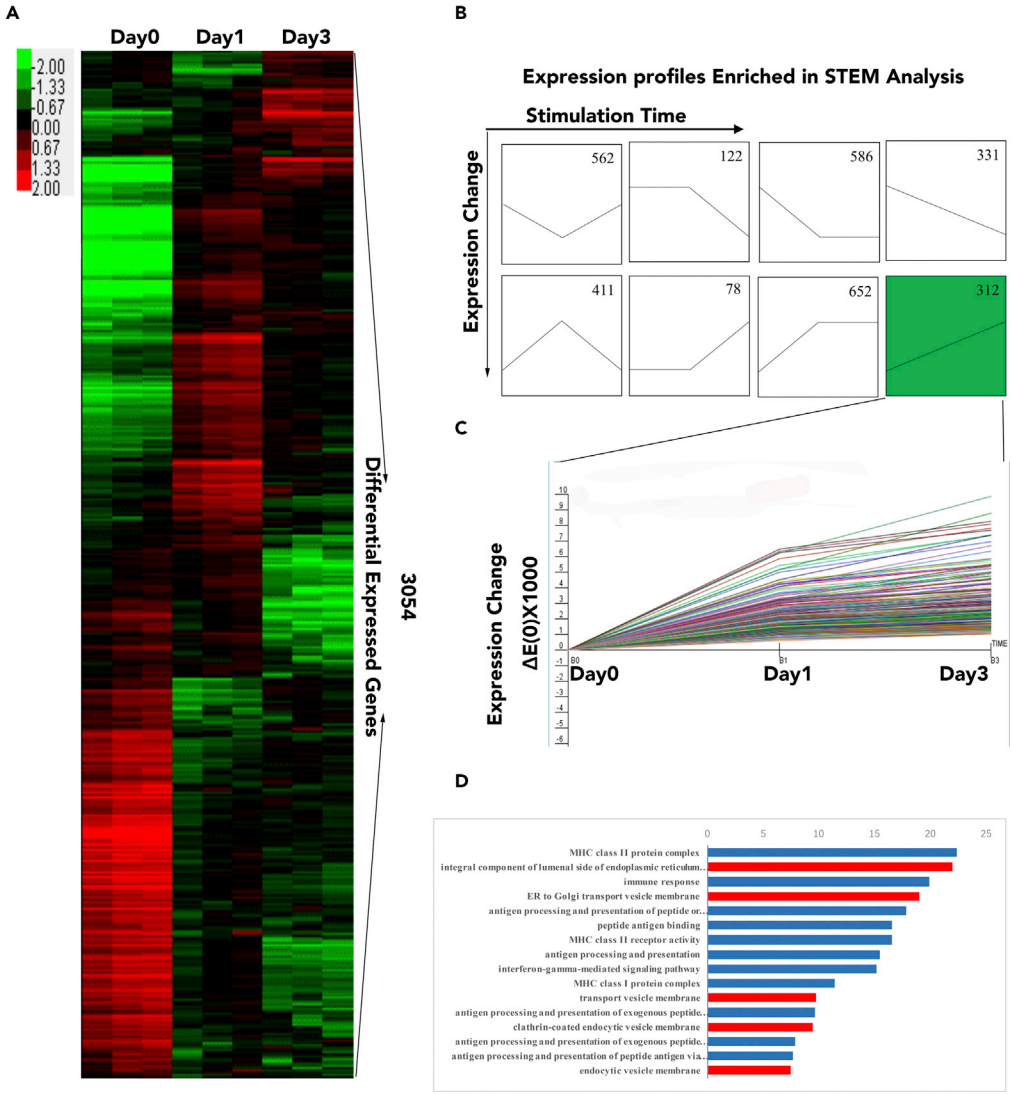

Figure 2. The Transcription Microarray Analysis of hESC-MSCs under IFN-γ Treatment

(A) The heatmap of differentially expressed genes between Day0, Day1, and Day3 hESC-MSCs.

(B) STEM analysis of all transcript levels differentially expressed genes between Day0, Day1, and Day3 hESC-MSCs. "n" represents the gene numbers of each profile.

(C) The STEM result of genes expression in the selected profile.

(D) Functional analysis of differentially expressed genes between Day0, Day1, and Day3 hESC-MSCs based on Gene Ontology. Blue bars indicate immune-activation-related GO; red bars indicate transportation-related GO.

MSCs Regulate HLA-I Endocytosis through the Clathrin-Independent Dynamin-Dependent Pathway

To determine the exact endocytosis pathway responsible for the regulation of HLA-I surface expression, we collected and applied several small molecules known to inhibit different endocytosis pathways (Figure 4A). Selected inhibitors were then separately applied on IFN-γ-stimulated hESC-MSCs where inhibitors marked as S8047 (dynasore, dynamin inhibitor) and S1342 (genistein, clathrin-independent inhibitor) were shown to lead to a significant increase in surface HLA-I expression; chloroquine, a lysosome inhibitor, also led to an upregulation of HLA-1 surface expression, but not as significant as S8047 and S1342. Other endocytosis and degeneration inhibitors showed very little or no effect on the cells' HLA-I surface expression (Figure 4B).

To further validate the influence of S1342 and S8047 on hESC-MSCs' HLA-I surface expression, cells were treated with a concentration gradient of these inhibitors. Data revealed that the application of S8047 or

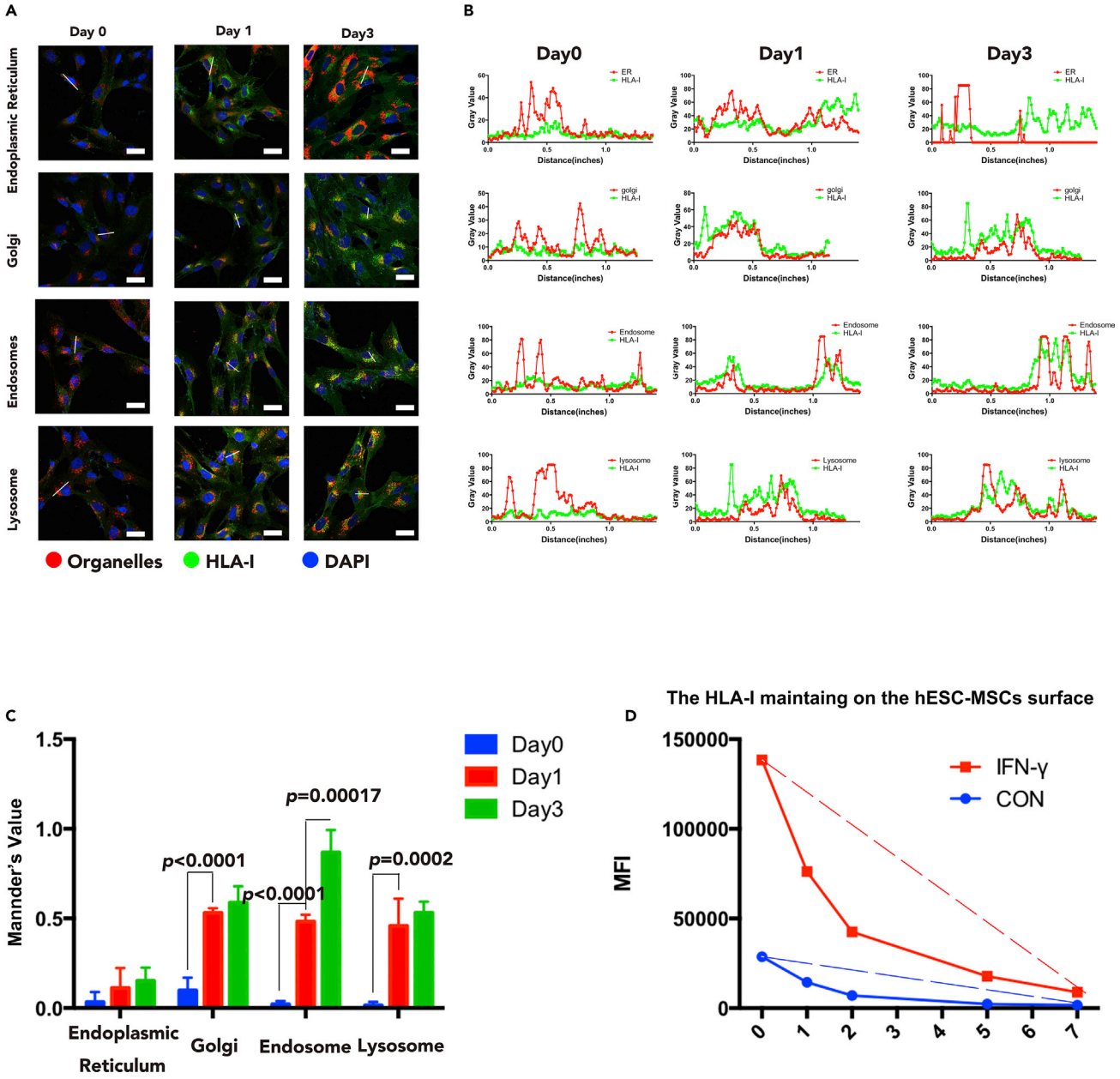

Figure 3. The Transportation of HLA-I in hESC-MSCs under IFN-γ Treatment

(A) HLA-I subcellular location in different organelles (including ER Golgi, endosome, and lysosome) of Day0, Day1, and Day3 hESC-MSCs. Red indicates organelles, green indicates HLA-I, and blue indicates DAPI. Scale bar, 50 μm.

(B) The immunofluorescence intensity analysis of HLA-I with different organelles in Day0, Day1, and Day3 hESC-MSCs (focused on the white line drawn on Figure 3A). The red line indicates organelles, and the green line indicates HLA-I.

(C) Mander's value analysis of co-localization rate of HLA-I and different organelles in Day1 and Day3 hESC-MSCs with the immunofluorescence results. n = 3 technical replicates. Data are shown as means ± SEM.

(D) HLA-I endocytosis analysis on hESC-MSCs with or without IFN-γ treatment by flow cytometry. The red line indicates IFN-γ-treated hESC-MSCs, and the blue line indicates IFN-γ-untreated hESC-MSCs; dashed line indicates the endocytosis rate of surface HLA-I.

S1342 at a higher dosage resulted in a stronger level of HLA-I surface expression (Figures 4C and 4D). Furthermore, the combination of S8047 and S1342 was detected to further upregulate the HLA-I surface expression when compared with a single inhibitor (Figure 4E). We also conducted a small interfering RNA experiment to knockdown DNM2 and RHOA, respectively, and data showed that both of them upregulate the surface HLA-I expression in the inflamed environment (Figures 4F and 4G). In conclusion, we

A

Target	Name	Selleck No.
Dynamin	Dynasore	S8047
Clathrin-dependent	Chlorpromazine	S2456
Clathrin-independent	Genistein	S1342
Caveola-mediated	Nystatin	S1934
Proteosome	MG-132	S2619
Lysosome	Chloroquine	

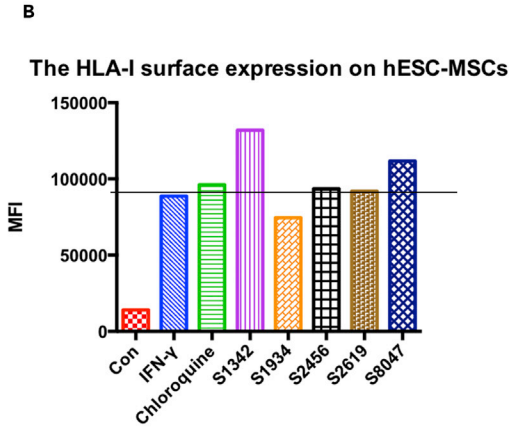

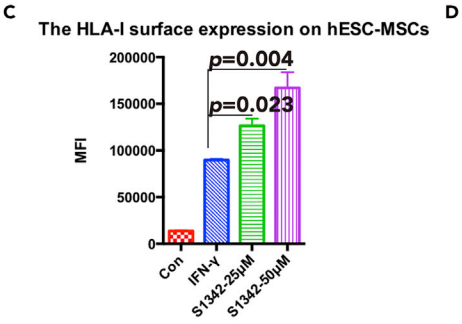

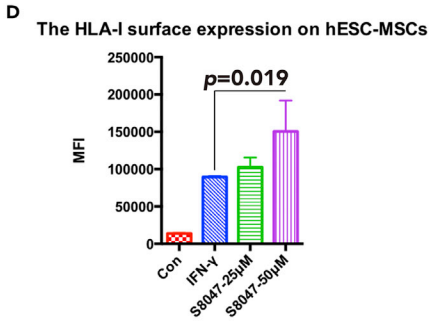

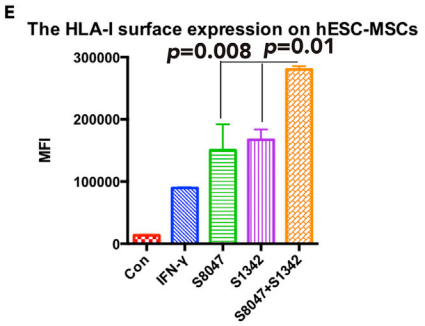

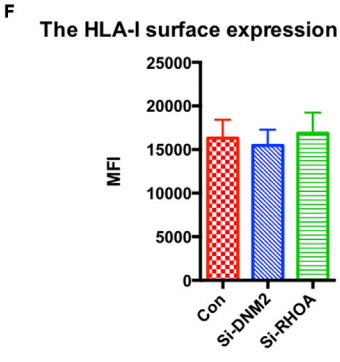

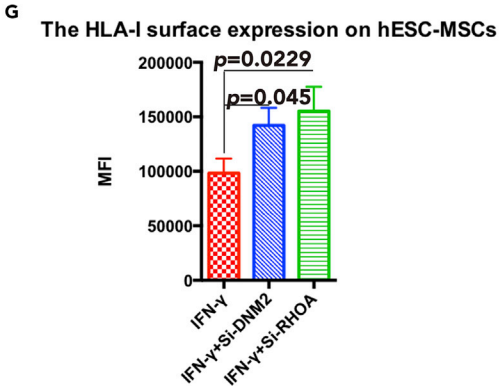

Figure 4. The Identification of the Selected Endocytosis Pathway for HLA-I in hESC-MSCs

(A) Summary of the selected inhibitors for different endocytosis pathways.

(B) The mean fluorescence index of HLA-I surface expression on hESC-MSCs with different inhibitor treatment was compared by flow cytometry analysis. The black dashed line indicates the compared hESC-MSCs group with only IFN-γ treatment. Data are shown as mean fluorescence index.

(C) The mean fluorescence index of HLA-I surface expression on IFN-γ-treated hESC-MSCs with different dosage of S1342 treatment was compared by flow cytometry analysis. Data are shown as means ± SEM.

(D) The mean fluorescence index of HLA-I surface expression on IFN-γ-treated hESC-MSCs with different dosage of S8047 treatment was compared by flow cytometry analysis. Data are shown as means ± SEM.

(E) The mean fluorescence index of HLA-I surface expression on IFN-γ-treated hESC-MSCs with the combination of S1342 and S8047 treatment was compared by flow cytometry analysis. Data are shown as means ± SEM.

Figure 4. *Continued*

(F) The mean fluorescence index of HLA-I surface expression on hESC-MSCs with different small interfering RNA (siRNA) transfection was compared by flow cytometry analysis. Data are shown as means ± SEM.

(G) The mean fluorescence index of HLA-I surface expression on IFN- γ-treated hESC-MSCs with different siRNA transfection was compared by flow cytometry analysis. Data are shown as means ± SEM.

suggest that hESC-MSCs regulate HLA-I endocytosis through the clathrin-independent and dynamin-dependent pathways.

The HLA-I Surface Expression Is Related with MSC Immunogenicity

To investigate whether the downregulation of surface HLA-I in hESC-MSCs is correlated with hESC-MSC immunogenicity, we applied a one-way mixed lymphocytes reaction culture to evaluate the immunogenicity of Day0, Day1, and Day3 hESC-MSCs. Allogeneic peripheral blood mononuclear cells (PBMCs) were stained with Carboxyfluorescein diacetate, succinimidyl ester (CFDA-SE) as responder cells to reflect the proliferation rate. Results illustrated that hESC-MSCs in all groups were able to induce allogenic PBMC proliferation to a certain extent; however, PBMCs stimulated with Day1 hESC-MSCs had fewer cells remaining in the unproliferated stage when compared with Day0 and Day3 hESC-MSCs (Figure 5A). The corresponding quantitative result indicated that the proliferation rate of PBMCs was the highest in the Day1 stimulation group, whereas that of the Day3 stimulation group was lower but still a little stronger than that of the Day0 group (Figure 5B).

We further developed a humanized $CD34^+$ mouse model to evaluate the immunogenicity of hESC-MSCs *in vivo*, imitating the human immune system. Immunodeficient mice (NSG) were first irradiated and then engrafted with human $CD34^+$ hematopoietic stem cells to be reconstituted with human lymphocytes lineages. At 6 weeks post-engraftment, we subcutaneously injected the DiI-labeled hESC-MSCs into the humanized mice; immunofluorescence staining results of hESC-MSCs revealed that these cells were able to retain in the host mice for 2 weeks, but the intensity varied between different groups (Figure 5C). Quantification analysis demonstrated that the immunofluorescence intensity of Day1 retained in the humanized mice was especially weaker than that of Day0 and Day3 groups (Figure 5D). In addition, we adopted the delayed-type hypersensitivity (DTH) test to assess T cell responses stimulated with different hESC-MSCs. The humanized mice were first primed with Day0, Day1, or Day3 hESC-MSCs for 2 weeks before the host mice were challenged with the same priming cells in footpads; thicker footpads signify a stronger T cell response reaction. DTH results showed that all hESC-MSCs with different HLA-I expressions were able to elicit allergic responses, whereas Day1 IFN-γ-stimulated cells induced a stronger immune response as reflected by the mice's thicker footpads compared with those of the other groups (Figure 5E). Consistently, histological H&E stainings revealed that the Day1-injected footpad exhibited more lymphocyte infiltration (Figure 5F). In summary, we compared the immunogenicity of Day0, Day1, and Day3 IFN-γ-treated hESC-MSCs, and the results suggested that hESC-MSC immunogenicity is consistent with HLA-I surface expression level.

DISCUSSION

Taken together, these data demonstrated that hESC-MSCs exhibited plasticity in the regulation of surface HLA-I expression under an inflamed environment. HLA-I molecules are expressed on all nucleated cells and play an important role in allogeneic rejection through their presentation of peptide antigens to $CD8^+$ T cells (Braciale, 1992), therefore a higher HLA-I expression on allogeneic cells will increase the risk of rejection by the host. Our results indicated that HLA-I expression levels varied in different cell types, with MSCs possessing a lower HLA-I surface expression when compared with somatic cells (Figures S2A–S2D). Previous studies have reported that MSCs showed low immunogenicity, including low expression of major histocompatibility complex (MHC) class I (also named HLA-I in human) and no expression of MHC class II and its co-stimulators CD40, CD80, and CD86 (Klyushnenkova et al., 2005). This phenomenon suggests that hESC-MSCs may be a universal off-the-shelf cell for MSC therapeutic applications. However, previous reports showed that the HLA-I expression level was also influenced by the different cell state and different cellular environment. We compared the HLA-I expression between hESC-MSCs at a late passage (slow cycle) and early passage (fast cycle) (Figure S3), where late-passage MSCs showed higher expression of HLA-I. Moreover, we also induced hESC-MSCs into quiescence by serum deprivation (SD) for 48 h and then compared their HLA-I surface expression with that of control hESC-MSCs in a standard culture condition; the result illustrated that there was more HLA-I expressed on cells in the SD group (Figure S4). These

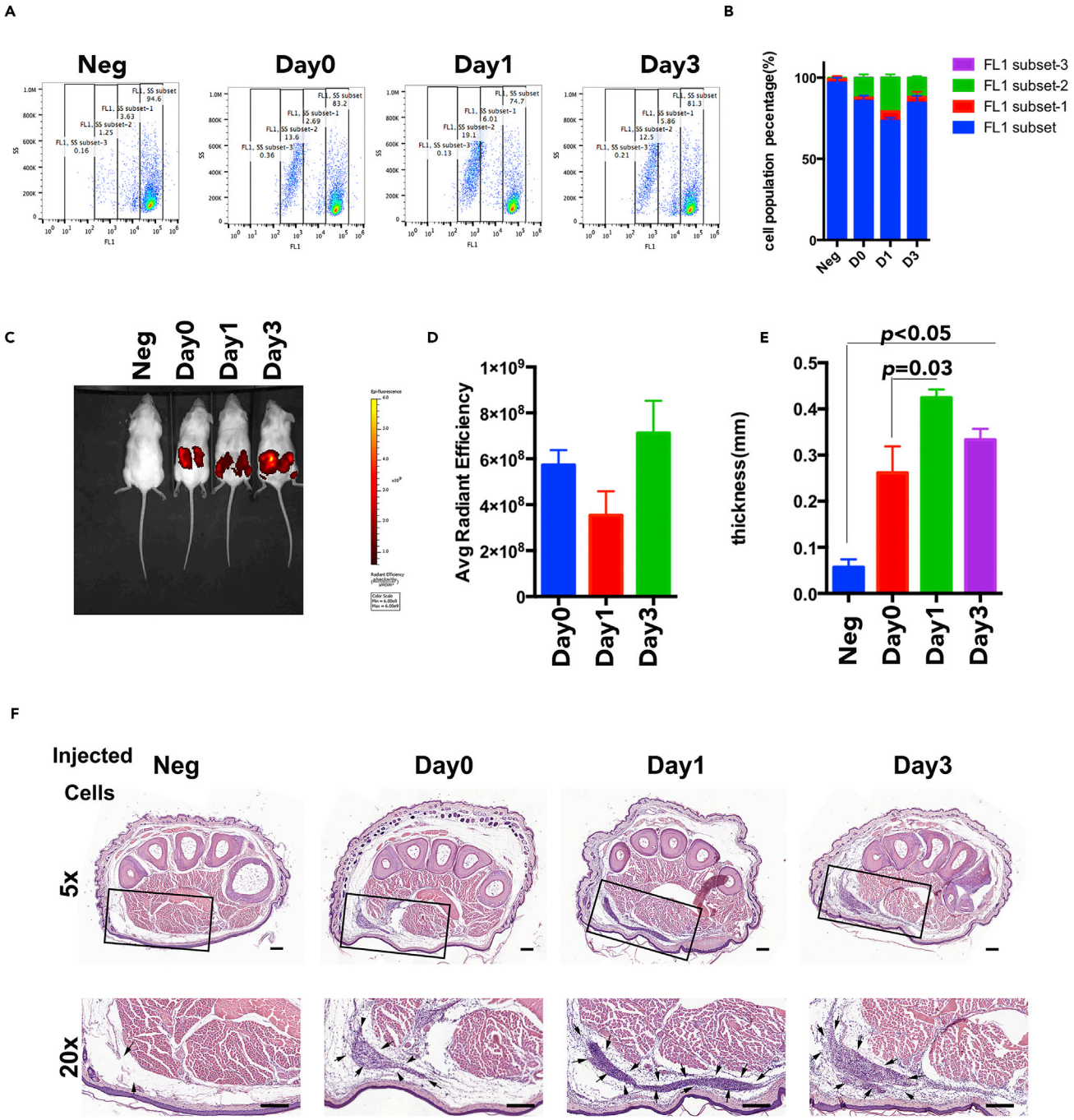

Figure 5. The Immunogenicity of hESC-MSCs with Day0, Day1, and Day3 hESC-MSCs

(A) PBMC proliferation rates with Day0, Day1, or Day3 hESC-MSC stimulation were compared by flow cytometry analysis. The FL1 subset indicates the non-proliferated PBMCs; the FL1 subset-1, FL1 subset-2, and FL1 subset-3 indicate the proliferated PBMCs; the PBMCs in later subset proliferate more times than the PBMCs in the former subset.

(B) PBMC proliferation rates with Day0, Day1, or Day3 hESC-MSC stimulation were quantified based on flow cytometry analysis. Data are shown as means ± SEM.

(C) Humanized mice imaging with Day0, Day1, or Day3 hESC-MSC injection after 2 weeks.

(D) The quantification analysis of Day0, Day1, or Day3 hESC-MSC immunofluorescence retained in humanized mice. Data are shown as means ± SEM.

(E) The footpad thickness of humanized mice with Day0, Day1, or Day3 hESC-MSC challenge. Data are shown as means ± SEM.

(F) The H&E staining of humanized mice footpads with Day0, Day1, or Day3 hESC-MSC challenge. The black arrows indicate the infiltrated lymphocytes in the footpad. Scale bar, 200 μm.

results are consistent with the outcome reported by Rumman et al. (Rumman et al., 2018), suggesting that MSCs express a higher surface level of HLA-I in the quiescent state. However, a study completed by Agudo et al. (Agudo et al., 2018) reported that HFSCs downregulate MHC-I in their quiescent state to evade immune surveillance. Thus MSCs and HFSCs had a different relationship between cell immunogenicity and the quiescent cell state. We suppose that this may be caused by the different types of stem cells: MSCs come from the mesenchyme, whereas HFSCs are from the epithelium. To MSCs there were no benefits but disadvantages, to maintain the quiescent state to downregulate HLA-I expression. When referring to the cellular microenvironment, IFN-γ plays a major role in multiple scenarios during immune activation; it is one of the most important pro-inflammatory cytokines produced primarily by NK cells, $CD4^+$T helper type 1 cells, cytotoxic $CD8^+$T cells, and dendritic cells, macrophages, and NK T cells (Eberl et al., 2015; Schroder et al., 2004), etc. Previous evidence indicated that IFN-γ could induce the immunosuppressive function of human MSCs, such as increasing the enzymatic activity of IDO1 or inhibiting $CD4^+$/$CD8^+$ T cell proliferation (Liotta et al., 2015; Sivanathan et al., 2014). Moreover, this cytokine has also been reported to upregulate MHC-I transcription level, which increased tumor immunogenicity (Weber and Rosenberg, 1988); this avenue of tumor surveillance was determined to involve recognition and elimination of tumor cells by cytotoxic T lymphocytes, recruited to the tumor mass via IFN-γ-induced chemokine signaling (Kunz et al., 1999). When considering MSCs, Chan et al. also found that IFN-γ markedly and instantly induced the expression of MHC-I in human bone marrow MSCs (Chan et al., 2008). However, it is still unclear whether IFN-γ treatment will have any impact on hESC-MSCs' immunogenicity.

Consistent with tumor cells and bone marrow MSCs (Martini et al., 2010; Saric et al., 2002), our results showed that IFN-γ treatment was able to constantly upregulate both HLA-I transcription and total protein levels. Interestingly, we observed that even though the HLA-I surface expression on hESC-MSCs was first upregulated, the expression level then auto-downregulated in the later stage; therefore this suggested that hESC-MSCs have the plasticity to maintain the level of HLA-I expression. However, recent reports have stated that MSCs' immunogenicity is influenced by multiple factors, including cell passages, donors' age, physiological status, and tissue sources. Comparing with our data on bone-marrow-derived MSCs (Figure S2A), we predicted that the autoregulating ability of MSCs' HLA-I surface expression may also be different between different sources of MSCs.

It has been reported that HIV-infected cells can downregulate the HLA-I surface expression by accelerating the ARF6 endocytic pathway (Blagoveshchenskaya et al., 2002), as well as blocking the transportation of HLA-I to the cell's surface (Swann et al., 2001). However, the mechanism of hESC-MSCs in modulating the downregulation of HLA-I surface expression is still unknown. Data obtained from our microarray analysis revealed a hint that the vesicle transport and endocytosis pathway may play a part in mediating the downregulation of HLA-I surface expression. To define which particular pathway was involved in the downregulation of HLA-I expression, we determined the location where HLA-I was overexpressed in the different subcellular fractions. We discovered a little amount of HLA-I co-localized within the ER, indicating that hESC-MSCs do not avoid HLA-I translocating onto the cell surface by restricting the molecules to ER, whereas plenty of HLA-I was found located in the Golgi, endosome, and lysosome. Moreover, the percentage of HLA-I located in the endosome and lysosome was found to be higher at Day3 when compared with Day1, indicating that the downregulation of surface HLA-I is mainly due to the endocytosis and degradation of HLA-I. Our flow cytometry results confirmed that HLA-I surface expression on hESC-MSCs was upregulated under IFN-γ treatment; however, these cells exhibited faster surface HLA-I endocytosis rate to maintain a low expression level of HLA-I.

Endocytosis, the process by which cells internalize macromolecules and surface proteins, involves several distinct pathways (Elkin et al., 2016) including clathrin-mediated endocytosis, caveolae-mediated endocytosis, and clathrin-independent endocytosis pathway. To identify the endocytosis pathway involved in hESC-MSCs' HLA-I expression regulation, we applied selective inhibitors of different pathways. When compared with the non-treated group, results illustrated an increase in HLA-I surface expression when inhibitors dynasore and genistin were applied; a higher dosage of these two inhibitors also resulted in higher surface expression of HLA-I. Moreover, the combination of these two inhibitors also resulted in a more efficient upregulation of HLA-I surface expression. The time series experiment implicated that both dynasore and genistin have the ability to block the downregulation of HLA-I surface expression on hESC-MSCs. These results all indicate that the HLA-I endocytosis in IFN-γ-treated hESC-MSCs goes through the clathrin-independent and dynamin-dependent endocytosis pathway.

HLA-I is one of the major molecules reflecting the graft cells' immunogenicity; however, we were not sure if the downregulation of HLA-I can exactly affect the cells' immunogenicity. Mixed lymphocytes culture assay has been considered as a traditional and superior method in predicting allograft rejection *in vitro*. We co-cultured CFDA-SE-stained PBMCs with Day0, Day1, and Day3 hESC-MSCs separately and then tested the proliferation rate of PBMCs. Flow cytometry results showed that Day1 hESC-MSCs induced the highest stimulation index when compared with other groups (Day0 and Day3). Furthermore, we applied the DTH model in humanized mice to evaluate cell-mediated immune responses associated with IFN-γ-stimulated hESC-MSCs stimulated at different time points. The mice challenged with Day1 hESC-MSCs showed a more robust response in footpad swelling assays compared with those challenged with Day0 and Day3 hESC-MSCs. Meanwhile, histological staining results revealed that mice footpads challenged with Day1 hESC-MSCs had a significantly higher lymphocyte infiltration compared with those challenged with Day0 and Day3 hESC-MSCs. All these results indicated the importance of HLA-I surface expression in inducing an allogeneic immune response, and the hESC-MSCs' ability in regulating HLA-I expression can exactly downregulate cell immunogenicity, and then reduce the risk of immune rejection.

In previous studies, researchers tried to use the gene editing method to modify HLA-I expression, either targeted disruption of B2M gene in ESC to minimize the cells' immunogenicity (Wang et al., 2015) or replacement of the classical HLA-I with minimally polymorphic HLA-E molecules to escape allogeneic responses (Gornalusse et al., 2017). Here we discovered that hESC-MSCs obtained the ability to downregulate HLA-I surface expression naturally, even when stressed under pulsed IFN-γ treatment (Figure S5). Referring to a previous study, the MSCs showed enhanced T cell suppression when they were preconditioned by incubating them with IFN-γ for 48 h (Le Blanc et al., 2003). Thus maybe we can take advantage of this special property by priming hESC-MSCs with an appropriate dosage of IFN-γ for a specific time duration to enhance their immune-suppressive capacity and also to maintain their low surface HLA-I expression to evade immune surveillance. This may push forward the application of MSCs in clinical trials.

In summary, we revealed the ability of hESC-MSCs in auto-downregulating the surface HLA-I expression with IFN-γ treatment. This behavior has been manifested to leave the cell with low immunogenicity. This discovery not only broadens our knowledge of hESC-MSCs but also provides a beneficial strategy to minimize the risk of rejection.

Limitations of the Study

This study focused on the plasticity of MSCs' immunogenicity, which determines the cells' survival in the allogeneic host. IFN-γ is an essential inflammatory cytokine, which has been identified to have the ability to strengthen the MSCs' immunomodulatory effect. So here we only focused on the IFN-γ simulated inflammatory environment, without considering other inflammatory cytokines or other specific disease microenvironment.

METHODS

All methods can be found in the accompanying Transparent Methods supplemental file.

SUPPLEMENTAL INFORMATION

Supplemental Information can be found online at https://doi.org/10.1016/j.isci.2019.04.011.

ACKNOWLEDGMENTS

This work was supported by the National Key Research and Development Program of China (No. 2017YFA0104902), the National Natural Science Foundation of China grants (31200739, 31470948), as well as sponsored by the China Scholarship Council and Fundamental Research Funds for the Central Universities.

The authors would like to thank Bone Marrow Transplantation Center, The First Affiliated Hospital, School of Medicine, Zhejiang University, Hangzhou, China, for kindly providing donor blood to reconstitute humanized mice; Core facilities, Zhejiang University School of Medicine for the technical support; Laboratory Animal Center, Zhejiang University for the administrative support; and Prof. Yiting Zhou and Prof. Qiming Sun for suggestion.

AUTHOR CONTRIBUTIONS

Y.W. designed the experiment, performed most experiments, analyzed the data, and wrote the manuscript. J.H., L.G., and D.Y. performed the animal experiment and histological staining. V.B. contributed to language polishing. C.A. helped with the microarray data analysis. J.D. performed some molecular experiments. H.H. provided the donor blood to reconstitute humanized mice. X.Z. provided materials including human embryonic stem cell lines. H.O. and H.L. provided most materials, all facilities, and financial support. H.L. provided the idea and approved the manuscript submission.

DECLARATION OF INTERESTS

The authors declare no competing interests.

Received: October 23, 2018
Revised: February 27, 2019
Accepted: April 6, 2019
Published: May 31, 2019

REFERENCES

Aggarwal, S., and Pittenger, M.F. (2005). Human mesenchymal stem cells modulate allogeneic immune cell responses. Blood *105*, 1815–1822.

Agudo, J., Park, E.S., Rose, S.A., Alibo, E., Sweeney, R., Dhainaut, M., Kobayashi, K.S., Sachidanandam, R., Baccarini, A., Merad, M., et al. (2018). Quiescent tissue stem cells evade immune surveillance. Immunity *48*, 271–285.e5.

Ankrum, J.A., Ong, J.F., and Karp, J.M. (2014). Mesenchymal stem cells: immune evasive, not immune privileged. Nat. Biotechnol. *32*, 252–260.

Barrachina, L., Remacha, A.R., Romero, A., Vazquez, F.J., Albareda, J., Prades, M., Ranera, B., Zaragoza, P., Martin-Burriel, I., and Rodellar, C. (2016). Effect of inflammatory environment on equine bone marrow derived mesenchymal stem cells immunogenicity and immunomodulatory properties. Vet. Immunol. Immunopathol. *171*, 57–65.

Beggs, K.J., Lyubimov, A., Borneman, J.N., Bartholomew, A., Moseley, A., Dodds, R., Archambault, M.P., Smith, A.K., and McIntosh, K.R. (2006). Immunologic consequences of multiple, high-dose administration of allogeneic mesenchymal stem cells to baboons. Cell Transplant. *15*, 711–721.

Berglund, A.K., Fortier, L.A., Antczak, D.F., and Schnabel, L.V. (2017). Immunoprivileged no more: measuring the immunogenicity of allogeneic adult mesenchymal stem cells. Stem Cell Res. Ther. *8*, 288.

Bjorkman, P.J., Saper, M.A., Samraoui, B., Bennett, W.S., Strominger, J.L., and Wiley, D.C. (1987). The foreign antigen binding site and T cell recognition regions of class I histocompatibility antigens. Nature *329*, 512–518.

Blagoveshchenskaya, A.D., Thomas, L., Feliciangeli, S.F., Hung, C.H., and Thomas, G. (2002). HIV-1 Nef downregulates MHC-I by a PACS-1- and PI3K-regulated ARF6 endocytic pathway. Cell *111*, 853–866.

Braciale, T.J. (1992). Antigen processing for presentation by MHC class I molecules. Curr. Opin. Immunol. *4*, 59–62.

Campoli, M., Chang, C.C., Oldford, S.A., Edgecombe, A.D., Drover, S., and Ferrone, S. (2004). HLA antigen changes in malignant tumors of mammary epithelial origin: molecular mechanisms and clinical implications. Breast Dis. *20*, 105–125.

Chan, W.K., Lau, A.S., Li, J.C., Law, H.K., Lau, Y.L., and Chan, G.C. (2008). MHC expression kinetics and immunogenicity of mesenchymal stromal cells after short-term IFN-gamma challenge. Exp. Hematol. *36*, 1545–1555.

Chin, M.H., Mason, M.J., Xie, W., Volinia, S., Singer, M., Peterson, C., Ambartsumyan, G., Aimiuwu, O., Richter, L., Zhang, J., et al. (2009). Induced pluripotent stem cells and embryonic stem cells are distinguished by gene expression signatures. Cell Stem Cell *5*, 111–123.

Doi, A., Park, I.H., Wen, B., Murakami, P., Aryee, M.J., Irizarry, R., Herb, B., Ladd-Acosta, C., Rho, J., Loewer, S., et al. (2009). Differential methylation of tissue- and cancer-specific CpG island shores distinguishes human induced pluripotent stem cells, embryonic stem cells and fibroblasts. Nat. Genet. *41*, 1350–1353.

Eberl, G., Colonna, M., Di Santo, J.P., and McKenzie, A.N. (2015). Innate lymphoid cells. Innate lymphoid cells: a new paradigm in immunology. Science *348*, aaa6566.

Elkin, S.R., Lakoduk, A.M., and Schmid, S.L. (2016). Endocytic pathways and endosomal trafficking: a primer. Wien. Med. Wochenschr. *166*, 196–204.

Gornalusse, G.G., Hirata, R.K., Funk, S.E., Riolobos, L., Lopes, V.S., Manske, G., Prunkard, D., Colunga, A.G., Hanafi, L.A., Clegg, D.O., et al. (2017). HLA-E-expressing pluripotent stem cells escape allogeneic responses and lysis by NK cells. Nat. Biotechnol. *35*, 765–772.

Gu, L.H., Zhang, T.T., Li, Y., Yan, H.J., Qi, H., and Li, F.R. (2015). Immunogenicity of allogeneic mesenchymal stem cells transplanted via different routes in diabetic rats. Cell. Mol. Immunol. *12*, 444–455.

Hematti, P. (2011). Human embryonic stem cell-derived mesenchymal progenitors: an overview. Methods Mol. Biol. *690*, 163–174.

Hentze, H., Graichen, R., and Colman, A. (2007). Cell therapy and the safety of embryonic stem cell-derived grafts. Trends Biotechnol. *25*, 24–32.

Hewitt, E.W. (2003). The MHC class I antigen presentation pathway: strategies for viral immune evasion. Immunology *110*, 163–169.

Hosseini, S., Taghiyar, L., Safari, F., and Baghaban Eslaminejad, M. (2018). Regenerative medicine applications of mesenchymal stem cells. Adv. Exp. Med. Biol. *1089*, 108–141.

Kim, M., Erickson, I.E., Huang, A.H., Garrity, S.T., Mauck, R.L., and Steinberg, D.R. (2018). Donor variation and optimization of human mesenchymal stem cells chondrogenesis in hyaluronic acid. Tissue Eng. Part A *24*, 1693–1703.

Klyushnenkova, E., Mosca, J.D., Zernetkina, V., Majumdar, M.K., Beggs, K.J., Simonetti, D.W., Deans, R.J., and McIntosh, K.R. (2005). T cell responses to allogeneic human mesenchymal stem cells: immunogenicity, tolerance, and suppression. J. Biomed. Sci. *12*, 47–57.

Kollnberger, S. (2016). The role of HLA-class I heavy-chain interactions with killer-cell immunoglobulin-like receptors in immune regulation. Crit. Rev. Immunol. *36*, 269–282.

Kunimatsu, R., Nakajima, K., Awada, T., Tsuka, Y., Abe, T., Ando, K., Hiraki, T., Kimura, A., and Tanimoto, K. (2018). Comparative characterization of stem cells from human exfoliated deciduous teeth, dental pulp, and bone marrow-derived mesenchymal stem cells. Biochem. Biophys. Res. Commun. *501*, 193–198.

Kunz, M., Toksoy, A., Goebeler, M., Engelhardt, E., Brocker, E., and Gillitzer, R. (1999). Strong expression of the lymphoattractant C-X-C chemokine Mig is associated with heavy infiltration of T cells in human malignant melanoma. J. Pathol. *189*, 552–558.

Le Blanc, K., Tammik, C., Rosendahl, K., Zetterberg, E., and Ringden, O. (2003). HLA expression and immunologic properties of

differentiated and undifferentiated mesenchymal stem cells. Exp. Hematol. *31*, 890–896.

Lee, M., Jeong, S.Y., Ha, J., Kim, M., Jin, H.J., Kwon, S.J., Chang, J.W., Choi, S.J., Oh, W., Yang, Y.S., et al. (2014). Low immunogenicity of allogeneic human umbilical cord blood-derived mesenchymal stem cells in vitro and in vivo. Biochem. Biophys. Res. Commun. *446*, 983–989.

Liotta, F., Querci, V., Mannelli, G., Santarlasci, V., Maggi, L., Capone, M., Rossi, M.C., Mazzoni, A., Cosmi, L., Romagnani, S., et al. (2015). Mesenchymal stem cells are enriched in head neck squamous cell carcinoma, correlates with tumour size and inhibit T-cell proliferation. Br. J. Cancer *112*, 745–754.

Martini, M., Testi, M.G., Pasetto, M., Picchio, M.C., Innamorati, G., Mazzocco, M., Ugel, S., Cingarlini, S., Bronte, V., Zanovello, P., et al. (2010). IFN-gamma-mediated upmodulation of MHC class I expression activates tumor-specific immune response in a mouse model of prostate cancer. Vaccine *28*, 3548–3557.

Moya, A., Larochette, N., Paquet, J., Deschepper, M., Bensidhoum, M., Izzo, V., Kroemer, G., Petite, H., and Logeart-Avramoglou, D. (2017). Quiescence preconditioned human multipotent stromal cells adopt a metabolic profile favorable for enhanced survival under ischemia. Stem Cells *35*, 181–196.

Okita, K., Ichisaka, T., and Yamanaka, S. (2007). Generation of germline-competent induced pluripotent stem cells. Nature *448*, 313–317.

Rumman, M., Majumder, A., Harkness, L., Venugopal, B., Vinay, M.B., Pillai, M.S., Kassem, M., and Dhawan, J. (2018). Induction of quiescence (G0) in bone marrow stromal stem cells enhances their stem cell characteristics. Stem Cell Res. *30*, 69–80.

Saric, T., Chang, S.C., Hattori, A., York, I.A., Markant, S., Rock, K.L., Tsujimoto, M., and Goldberg, A.L. (2002). An IFN-gamma-induced aminopeptidase in the ER, ERAP1, trims precursors to MHC class I-presented peptides. Nat. Immunol. *3*, 1169–1176.

Schroder, K., Hertzog, P.J., Ravasi, T., and Hume, D.A. (2004). Interferon-gamma: an overview of signals, mechanisms and functions. J. Leukoc. Biol. *75*, 163–189.

Sivanathan, K.N., Gronthos, S., Rojas-Canales, D., Thierry, B., and Coates, P.T. (2014). Interferon-gamma modification of mesenchymal stem cells: implications of autologous and allogeneic mesenchymal stem cell therapy in allotransplantation. Stem Cell Rev. *10*, 351–375.

Swann, S.A., Williams, M., Story, C.M., Bobbitt, K.R., Fleis, R., and Collins, K.L. (2001). HIV-1 Nef blocks transport of MHC class I molecules to the cell surface via a PI 3-kinase-dependent pathway. Virology *282*, 267–277.

Wang, D., Quan, Y., Yan, Q., Morales, J.E., and Wetsel, R.A. (2015). Target disruption of b2m gene minimizes the immunogenicity of human embryonic stem cells. Stem Cells Transl. Med. *4*, 1234–1245.

Wang, L.T., Ting, C.H., Yen, M.L., Liu, K.J., Sytwu, H.K., Wu, K.K., and Yen, B.L. (2016). Human mesenchymal stem cells (MSCs) for treatment towards immune- and inflammation-mediated diseases: review of current clinical trials. J. Biomed. Sci. *23*, 76.

Wang, Y., Yu, D., Liu, Z., Zhou, F., Dai, J., Wu, B., Zhou, J., Heng, B.C., Zou, X.H., Ouyang, H., et al. (2017). Exosomes from embryonic mesenchymal stem cells alleviate osteoarthritis through balancing synthesis and degradation of cartilage extracellular matrix. Stem Cell Res. Ther. *8*, 189.

Weber, J.S., and Rosenberg, S.A. (1988). Modulation of murine tumor major histocompatibility antigens by cytokines in vivo and in vitro. Cancer Res. *48*, 5818–5824.

Yang, X.F., Chen, T., Ren, L.W., Yang, L., Qi, H., and Li, F.R. (2017). Immunogenicity of insulin-producing cells derived from human umbilical cord mesenchymal stem cells. Exp. Ther. Med. *13*, 1456–1464.

Yang, Y.K., Ogando, C.R., Wang See, C., Chang, T.Y., and Barabino, G.A. (2018). Changes in phenotype and differentiation potential of human mesenchymal stem cells aging in vitro. Stem Cell Res Ther. *9*, 131.

Yu, J., Vodyanik, M.A., Smuga-Otto, K., Antosiewicz-Bourget, J., Frane, J.L., Tian, S., Nie, J., Jonsdottir, G.A., Ruotti, V., Stewart, R., et al. (2007). Induced pluripotent stem cell lines derived from human somatic cells. Science *318*, 1917–1920.

Zangi, L., Margalit, R., Reich-Zeliger, S., Bachar-Lustig, E., Beilhack, A., Negrin, R., and Reisner, Y. (2009). Direct imaging of immune rejection and memory induction by allogeneic mesenchymal stromal cells. Stem Cells *27*, 2865–2874.

ISCI, Volume *15*

Supplemental Information

The Plasticity of Mesenchymal Stem Cells in Regulating Surface HLA-I

Yafei Wang, Jiayun Huang, Lin Gong, Dongsheng Yu, Chenrui An, Varitsara Bunpetch, Jun Dai, He Huang, Xiaohui Zou, Hongwei Ouyang, and Hua Liu

Transparent Methods

Ethics Statement

All experiments were approved by the institutional biosafety committee, institutional animal committee, and institutional review board of Zhejiang University. (No. ZJU2015-004)

Cell culture and Differentiation

The male H1 human ES cell line (ESC) was obtained from WiCell Corporation. Madison, WI, USA (http://www.wicell.org), and was maintained in the undifferentiated state in a feeder-free system. MSCs derived from ESC (hESC-MSCs) were directly differentiated, cultured, and identified as described in our previous study(Wang et al., 2017). In addition, the hESC-MSCs was normally cultured in standard conditions (L-DMEM within 10%FBS). However, for the serum deprivation experiment, the cells were seeded 10000 cells per cm^2 and cultured under standard conditions over night. The following day, cells were rinsed with PBS and further cultured in L-DMEM with 5%FBS or L-DMEM without FBS for 48h, respectively.

Cell stimulation

The hESC-MSCs were stimulated with 100U/mL IFN-γ(PeproTech, Cat.300-02) in MSC culture media (L-DMEM+10%FBS) for 0 days, 1 day, 2 days, and 3 days, and then directly used for the following experiment(Figure S6A). The sample was marked as Day0, Day1, Day2, and Day3. As for the pulsative IFN-γ stimulation, the hESC-MSCs medium was transferred between medium within and without 100U/mL IFN-γ (Figure S6B).

One-way mixed lymphocyte culture

Human PBMCs were prepared from freshly collected, heparinized whole blood samples from donors through Ficoll-Paque PLUS (GE, Cat.17-1440-03). Briefly, whole human blood was diluted 1:2 with PBS and added into the Ficoll solution at 4:3(v/v) ratio. After centrifugation and washing, PBMCs were stained with CFDA SE (Beytime, Cat.C1031) to label the cell proliferation used as responder cells. The hESC-MSCs were then treated with 25μg/mL Mitomycin C used as stimulator cells. 10^4 stimulator cells and 10^5 responder cells were co-cultured into a 96-well round-bottom plate (Corning) for 5 days. PBMCs proliferation was then analyzed with the fluorescence intensity by flow cytometry.

Reconstitution of humanized mice

The B-NDG mice (NOD-scid IL2 receptor gamma null mice) were purchased from Biocytogen

Jiangsu Co., Ltd (Jiangsu, China) at 5 weeks of age. Human $CD34^+$ cells were extracted from the donor blood through Ficoll-Paque PLUS (GE, Cat.17-1440-03) which is supplied by Bone Marrow Transplantation Center, The First Affiliated Hospital, School of Medicine, Zhejiang University, Hangzhou, China. Humanized mice were generated as previously described(Pearson et al., 2008). Briefly, the B-NDG mice were first treated with sublethal irradiation (1.8 Gy), then 5×10^5 human $CD34^+$ cells were intravenously injected into the mice 5 hours later. The $CD34^+$ cells were isolated purified from human PBMCs using a MACS separation system with anti-human $CD34^+$ antibody (Miltenyi Biotec, Cat. 130-046-702). After 6 weeks, the mice were delivered to do the following experiment.

Delayed-type hypersensitivity

Humanized mice were injected subcutaneously with 200 μL 1×10^6 DiI (Beyotime, Cat.C1036) pre-stained hESC-MSCs (Day0, Day1, and Day3) at two sites on the back of the mice (priming). At 13 days after post-implantation, the mice were detected with immunofluorescence through In Vivo Imaging System (PE, IVIS Spectrum). 1×10^6 challenged hESC-MSCs (Day0, Day1, and Day3) in 20μL of PBS were injected into one hind footpad of humanized mice subcutaneously (challenge). Another 20μL of PBS were injected into the other hind footpad of humanized mice subcutaneously as the internal negative control. Evaluation of the responses was performed as previously described(Liu et al., 2012): [footpad swelling (mm)]=[footpad thickness of hESC-MSCs injected footpad (mm)]-[footpad thickness of PBS injected footpad (mm)].

H&E staining of the footpad

At 24 hours post-challenge, humanized mice footpads of all groups were harvested and fixed in 4% paraformaldehyde. After decalcification in 10% EDTA at 4℃ for 4 weeks, footpads were cross-sectioned at the root of toes before paraffin embedding. Sections of 4μm thickness were made and stained with H&E. Images were captured under the slide scanning machine (Pannoramic MIDI, 3DHISTECH Ltd., Budapest, Hungray).

Transfection of small interfering RNAs

The siRNA sequences used in this study are as follows:siRNA-DNM2 (forward: 5'-GCAACCUGGUGGACUCAUATT-3', reverse: 5'-UAUGAGUCCACCAGGUUGCTT-3'); si-RHOA (forward: 5'-CCAGAAGUCAAGCAUUUCUTT-3', reverse: 5'-

AGAAAUGCUUGACUUCUGGTT-3'); si-Negative Control (forward: 5'-UUCUCCGAACGUGUCACGUTT-3', reverse: 5'-ACGUGACACGUUCGGAGAATT-3'). Double-stranded siRNAs were synthesized by GenePharma. The reaction contained 100nM siRNAs, and transfections were performed using Lipofectamine^{TM}2000 Transfection Reagent (Invitrogen, Cat.11668019) . after 6 hours, the transfected cells were then refreshed with MSC medium.

Quantitative real-time polymerase chain reaction (qRT-PCR)

Total RNA was isolated from hESC-MSCs by lysis in TRIzol (Takara, Shigo, Japan, Cat. #9109). Rever-Tra Ace qPCR RT Master Mix was applied during the reverse transcription process (Toyobo, Osaka, Japan, Cat. #FSQ-201). qRT-PCR was performed utilizing Brilliant SYBR Green QPCR Master Mix (Takara, Cat. # RR420A) with a LightCycler apparatus (480II, Roche, Mannheim, Germany). The amplification efficiencies of primer pairs were validated to enable quantitative comparison of gene expression. All primer sequences (Invitrogen) were designed using Primer 5.0 software (Table S1). Each qRT-PCR was performed three times on at least three different experimental replicates, and results were normalized to those obtained with the endogenous reference gene (GAPDH).

Western blot assay

Cellular protein was extracted with RIPA lysis buffer (Solarbio, Beijing, China, Cat. #R0010), and the total protein concentration was determined with a BCA Protein Assay Kit (Pierce, Rockford, IL, USA, Cat. #23225). The 20 μg extracted cellular protein was loaded on 10% (w/v) SDS-PAGE-denaturing gels. After electrophoresis, proteins were transferred to a polyvinylidene difluoride membrane and blocked in 5% (w/v) bovine serum albumin (BSA, Sangon Biotech, Shanghai, China, Cat. #9048-4b-8) for 1h at room temperature. The membrane was incubated overnight at 4 °C with mouse anti-HLA-I (1:1000; HLA-ABC, Novus, Cat.NB100-64775), or rabbit anti-GAPDH (1:1000; Beyotime, Cat. #AG019) antibody. After washing in Tris-buffered saline with Tween-20 (TBST), the horseradish peroxidase (HRP) secondary antibodies (HRP-labeled goat anti-mouse IgG (1:1000; Beyotime, Cat. #A0216) and goat anti-rabbit IgG antibody, peroxidase-conjugated (1:1000; EMD Millipore, Cat. #AP132P)) was diluted in 5% (w/v) BSA solution and incubated accordingly with the membrane for 1 h at room temperature (RT). The excessive secondary antibody was washed off by TBST, and a

chemiluminescent signal was generated by the ECL Imaging Kit (Thermo Fisher Scientific, Waltham, MA, USA, Cat. #32209).

Flow cytometry

Cells were harvested by trypsinization (0.05% (w/v); Life Technologies, Cat. #15400-054) for 2 min in a 37℃ incubator, and the cell pellet was re-suspended in PBS to a titer of 10^5/10 μL. The cell suspension was incubated with 10μL anti-HLA-I (1:30; HLA-ABC, Novus, Cat.NB100-64775) on ice for 30min. Cells were washed with PBS completely and incubated with 40μL anti-mouse Alexa Fluor 488(1:250; Donkey anti-Mouse IgG (H+L) Highly Cross-Adsorbed Secondary Antibody, Alexa Fluor 488, Invitrogen, Cat. A-21202) on ice for 15min. Cells were washed with PBS completely and re-suspended in 1% (w/v) paraformaldehyde. Samples were run on the FC500MPL flow cytometer (Beckman Coulter, Brea, CA, USA) and the data were analyzed by FlowJo vX.0.7 software (FlowJo LLC, Ashland, OR, USA).

RNA extraction and preparation

Total RNA containing small RNA was extracted from IFN-γ-treated hESC-MSC samples using the Trizol reagent (Invitrogen) and purified with mirVana miRNA Isolation Kit (Ambion, Austin, TX, USA) according to manufacturer's protocol. The purity and concentration of RNA were determined from OD260/280 readings using the spectrophotometer (NanoDrop ND-1000). RNA integrity was determined by 1% formaldehyde denaturing gel electrophoresis. Only RNA extracts with RNA integrity number values >6 were used for further study.

Fabrication of DNA microarray

CapitalBio Technology Human LncRNA Array v4 was designed with four identical arrays per slide (4 x 180K format), with each array containing probes interrogating about 41,000 human lncRNAs and about 34,000 human mRNAs. Those lncRNA and mRNA target sequences were merged from multiple databases, 23898 from GENCODE/ENSEMBL, 14353 from Human LincRNA Catalog(Orom et al., 2010), 7760 from RefSeq, 5627 from UCSC, 13701 from NRED (ncRNA Expression Database), 21488 from LNCipedia, 1038 from H-InvDB, 3019 from LncRNAs-a (Enhancer-like), 1053 from Antisense lncRNA pipeline, 407 Hox ncRNAs, 962 UCRs, and 848 from Chen Ruisheng lab (Institute of Biophysics, Chinese Academy of Science). Each RNA was detected by probes twice. The array also contains 4974 Agilent control probes.

Microarray imaging and data analysis

The lncRNA+mRNA array data were analyzed for data summarization, normalization, and quality control using the GeneSpring software V13.0 (Agilent). To select the differentially expressed genes, we used threshold values of ≥2 and ≤−2-fold change and a Benjamini-Hochberg corrected p-value of 0.05. The data was Log2 transformed and median centered by genes using the Adjust Data function of CLUSTER 3.0 software, then further analyzed with hierarchical clustering with average linkage. Finally, we selected mRNAs with differentiated expression to perform short time series expression miner (STEM) analysis(Ernst and Bar-Joseph, 2006). Genes classified in eight model profiles were further analyzed with DAVID.

Flow cytometry analysis to assay endocytosis rate

To detect the HLA-I endocytosis rate of hESC-MSCs, cells were harvested by trypsinization (0.05% (w/v); Life Technologies, Cat. #15400-054) for 2 min, and the cell pellet was re-suspended in PBS to a titer of 10^6/100μL. The cell suspension was incubated with 100μL of HLA-ABC (1:25, Novus, Cat.NB100-64775) for 30min on ice. Cells were washed with PBS completely and resuspended in 50μL. The sample was divided into 5 parts: 0h, 1h, 2h, 5h, 7h. Cells were added in 1000μL cell medium and put back into the incubator to initiate endocytosis (37℃,5% CO2). At a certain time point, cells were put on the ice to stop the endocytosis process. Cell samples were harvested and centrifuged at 200× g, 5min, before resuspension in 40μL anti-mouse Alexa Fluor 488(1:250; Donkey anti-Mouse IgG (H+L) Highly Cross-Adsorbed Secondary Antibody, Alexa Fluor 488, Invitrogen, Cat. A-21202) on ice for 15min. Cells were then washed with PBS and re-suspended in 1% (w/v) paraformaldehyde. Samples were run on an FC500MPL flow cytometer (Beckman Coulter, Brea, CA, USA) and the data were analyzed by FlowJo vX.0.7 software (FlowJo LLC, Ashland, OR, USA).

Statistical analysis

All data were expressed as mean ± SEM unless otherwise stated. All experiments in vitro were repeated independently at least twice in addition to the triplicates applied in each experiment. Statistical results were analyzed and bar charts were constructed with GraphPad Prism version 5.0 (GraphPad Software, San Diego, CA, USA). Statistical results were considered significant when the p-value was less than 0.05. Two-tailed Student's t-test was used to compare two groups at the same time point. One-way ANOVA including the Tukey-Kramer post hoc test was

used to compare multiple time point groups.

Data and software available

The accession number for microarray data reported in this paper is GEO Database: GSE122091.

Reference

Ernst, J., and Bar-Joseph, Z. (2006). STEM: a tool for the analysis of short time series gene expression data. BMC Bioinformatics *7*, 191.

Liu, H., Lu, K., MacAry, P.A., Wong, K.L., Heng, A., Cao, T., and Kemeny, D.M. (2012). Soluble molecules are key in maintaining the immunomodulatory activity of murine mesenchymal stromal cells. Journal of cell science *125*, 200-208.

Orom, U.A., Derrien, T., Beringer, M., Gumireddy, K., Gardini, A., Bussotti, G., Lai, F., Zytnicki, M., Notredame, C., Huang, Q.*, et al.* (2010). Long noncoding RNAs with enhancer-like function in human cells. Cell *143*, 46-58.

Pearson, T., Greiner, D.L., and Shultz, L.D. (2008). Creation of "humanized" mice to study human immunity. Current protocols in immunology / edited by John E Coligan [et al] *Chapter 15*, Unit 15 21.

Wang, Y., Yu, D., Liu, Z., Zhou, F., Dai, J., Wu, B., Zhou, J., Heng, B.C., Zou, X.H., Ouyang, H.*, et al.* (2017). Exosomes from embryonic mesenchymal stem cells alleviate osteoarthritis through balancing synthesis and degradation of cartilage extracellular matrix. Stem Cell Res Ther *8*, 189.

Supplemental Figure Titles and Legends

Figure S1. The HLA-I surface expression on hBMSCs under IFN-γ treatment, related to Figure 1.

(A) HLA-I surface expression on hBMSCs (red line) within IFN-γ treatment for 0 day, 1 day, 2 days and 3 days were compared by flow cytometry analysis. Blue line demarcates isotype control.

(B) The flow cytometry results quantified analysis of HLA-I surface expression level on hBMSCs with IFN-γ treatment for 0 day, 1 day, 2 days and 3 days by mean fluorescence index. Data are shown as means±SEM.

Figure S2. HLA-I levels are lower in hESC-MSCs than hFF, related to Figure 1.

(A) qRT-PCR expression analysis of HLA-I related genes (include HLA-A, HLA-B, HLA-C, and B2M) on hESC-MSCs and hFF. RNA expression levels were normalized to the level of GAPDH expression. Data are shown as means±SEM.

(B) HLA-I expression in hESC-MSCs and hFF were compared by western blotting.

(C) HLA-I surface expression level on hESC-MSCs (red line) and hFF (blue line) were compared by flow cytometry analysis. Dashed lines demarcate isotype control.

(D) The flow cytometry results quantified analysis of HLA-I surface expression level on hESC-MSCs (red bar) and hFF (blue bar) with mean fluorescence index. Data are shown as means±SEM.

Figure S3. HLA-I levels are lower in hESC-MSCs at early passage than hESC-MSCs at late passage, related to Figure 1.

(A) hESC-MSCs growth curve at different passage(from passage0 to passage9).

(B) The flow cytometry results quantified analysis of HLA-I surface expression level on passage3 hESC-MSCs (red bar) and passage8 hESC-MSCs(blue bar) with mean fluorescence index. Data are shown as means±SEM.

Figure S4. HLA-I levels are higher in hESC-MSCs after the serum deprivation, related to Figure 1.

(A) HLA-I surface expression level on hESC-MSCs under different concentration of FBS treatment for 48h was compared by flow cytometry analysis. The blue lines demarcate isotype control.

(B) The flow cytometry results quantified analysis of HLA-I surface expression level on 10%FBS treated hESC-MSCs (red bar), 5%FBS treated hESC-MSCs(blue bar), and 0%FBS treated hESC-MSCs(green bar) with mean fluorescence index. Data are shown as means±SEM.

Figure S5. HLA-I levels in hESC-MSCs within pulsed IFN-γ treatment, related to Figure 1.

(A) HLA-I surface expression level on hESC-MSCs under pulsed IFN-γ treatment was compared by flow cytometry analysis. The blue lines demarcate isotype control.

(B) The flow cytometry results quantified analysis of HLA-I surface expression level on hESC-MSCs under pulsed IFN-γ treatment with mean fluorescence index. Data are shown as means±SEM.

Figure S6. Schematic diagram of the collection about hESC-MSCs under IFN-γ treatment, related to Figure 1 and Figure S5.

(A) The Schematic diagram of the collection about hESC-MSCs under continuous constant IFN-γ treatment.

(B) The Schematic diagram of h the collection about hESC-MSCs under pulsed IFN-γ treatment.

Table S1. The primers designed for qRT-PCR, related to Figure 1 and Figure S2.

Gene	Sequence(5'-3')
HLA-A-F	TCCTTGGAGCTGTGATCACT
HLA-A-R	AAGGGCAGGAACAACTCTTG
HLA-B-F	ATTACATCGCCCTGAACGAG
HLA-B-R	ATCTCCGCAGGGTAGAAACC
HLA-C-F	TCCTGGTTGTCCTAGCTGTC
HLA-C-R	CAGGCTTTACAAGTGATGAG
B2M-F	GATGAGTATGCCTGCCGTGTG
B2M-R	CAATCCAAATGCGGCATCT
GAPDH-F	TGACGCTGGGGCTGGCATTG
GAPDH-R	GGCTGGTGGTCCAGGGGTCT

Figure S1

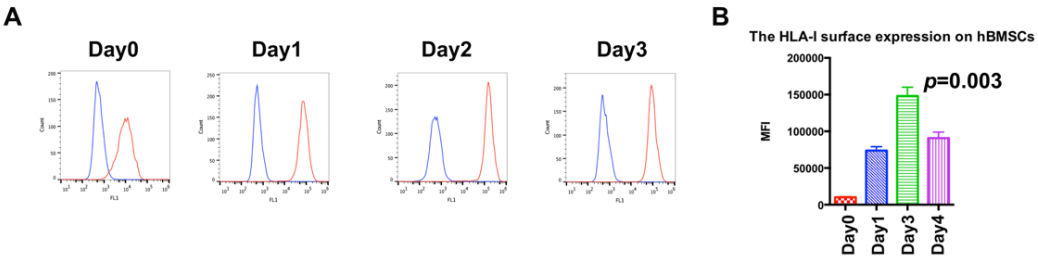
A
Day0
Day1
Day2
Day3
B
The HLA-I surface expression on hBMSCs
MFI
200000
150000
100000
50000
0
p=0.003
Day0
Day1
Day3
Day4

Figure S2

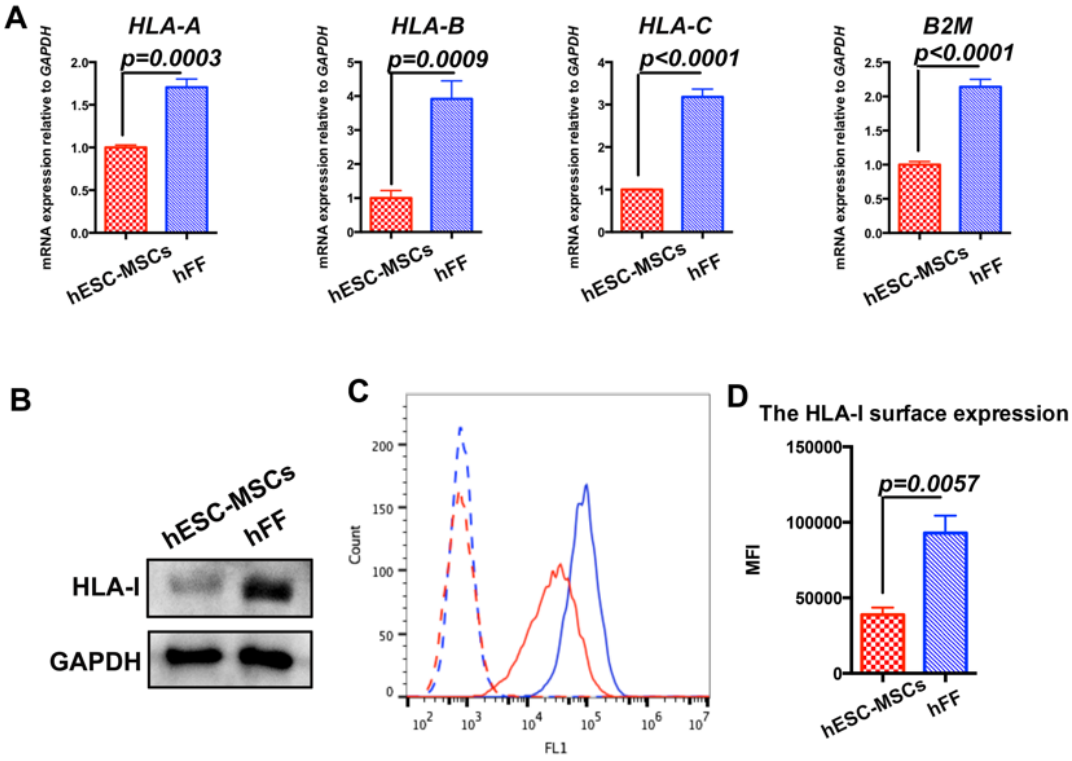
A
HLA-A
p=0.0003
HLA-B
p=0.0009
HLA-C
p<0.0001
B2M
p<0.0001
mRNA expression relative to GAPDH
hESC-MSCs
hFF
B
hESC-MSCs
hFF
HLA-I
GAPDH
C
Count
FL1
D
The HLA-I surface expression
MFI
p=0.0057

Figure S3

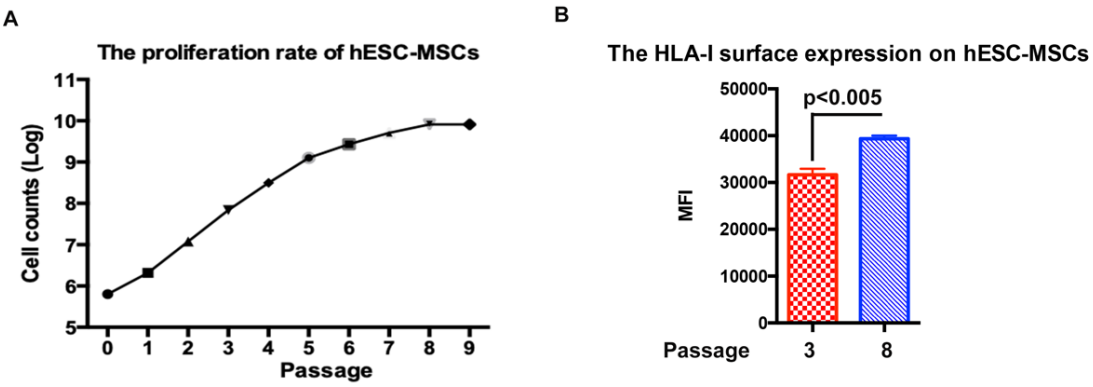
A
The proliferation rate of hESC-MSCs
Cell counts (Log)
11
10
9
8
7
6
5
0 1 2 3 4 5 6 7 8 9
Passage
B
The HLA-I surface expression on hESC-MSCs
p<0.005
MFI
50000
40000
30000
20000
10000
0
Passage
3
8

Figure S4

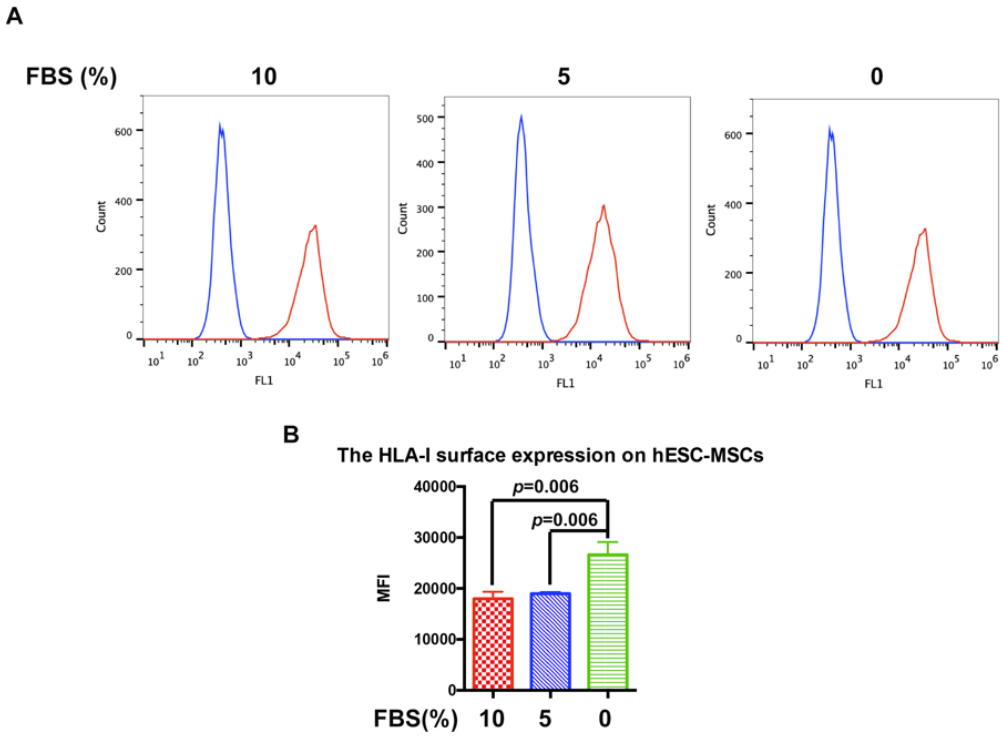
A
FBS (%)
10
5
0
Count
FL1
B
The HLA-I surface expression on hESC-MSCs
p=0.006
p=0.006
MFI
FBS(%) 10 5 0

Figure S5

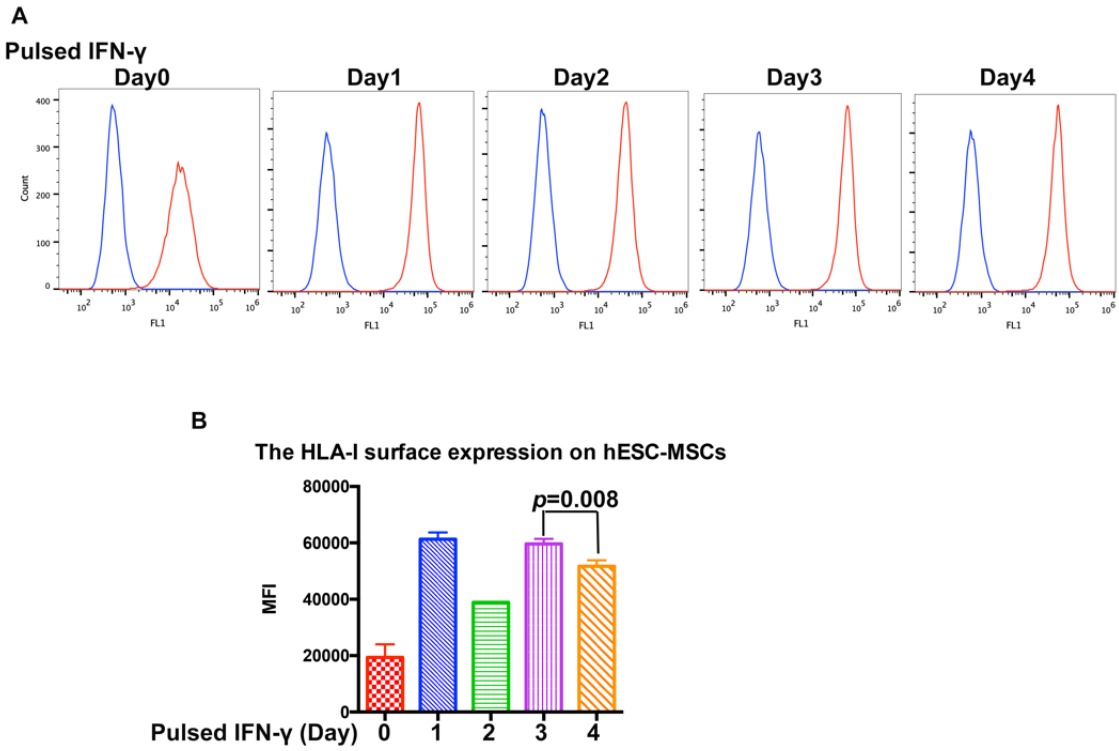
A
Pulsed IFN-γ
Day0
Day1
Day2
Day3
Day4
Count
FL1
B
The HLA-I surface expression on hESC-MSCs
MFI
p=0.008
80000
60000
40000
20000
0
Pulsed IFN-γ (Day) 0 1 2 3 4

Figure S6

A

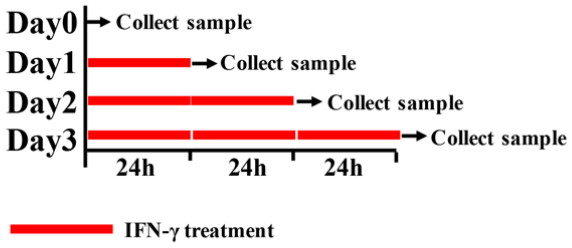
Day0
Collect sample
Day1
Collect sample
Day2
Collect sample
Day3
Collect sample
24h
24h
24h
IFN-γ treatment

B

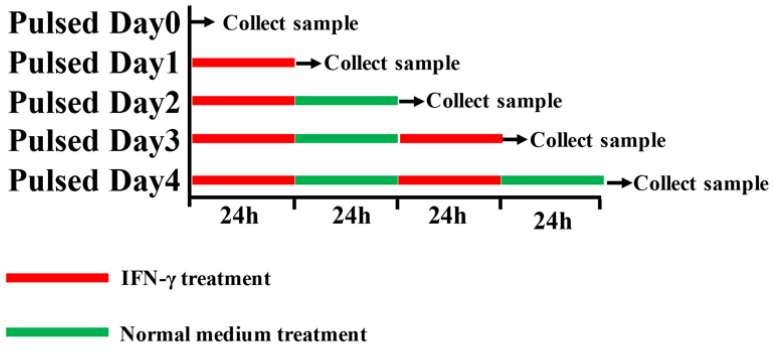
Pulsed Day0
Collect sample
Pulsed Day1
Collect sample
Pulsed Day2
Collect sample
Pulsed Day3
Collect sample
Pulsed Day4
Collect sample
24h
24h
24h
24h
IFN-γ treatment
Normal medium treatment